Journal of Mechanical Engineering Research and Developments
ISSN: 1024-1752
CODEN: JERDFO
Vol. 43, No. 4, pp. 193-206
Published Year 2020

Investigate the Flatson Wear and Rolling Contact Fatigue of Wheel Materials

Adel M Bash[†]*, Hassan A. Abdulhadi[‡] and Sulaiman E. Mnawe[†]

[†]Department of Mechanical Engineering, College of Engineering, University of Tikrit, Tikrit, Iraq

[‡]Middle Technical University, Institute of Technology, Baghdad 10074, Iraq

*Email: adelbash@tu.edu.iq

ABSTRACT: The rapid development of high-speed railways led to wheel damage. This problem was more prominent at wheel abrasion, which is a more serious type of wheel damage. Therefore, to ensure the safe operation of the vehicle, the study of the formation process of the wheel abrasion and the influence of the abrasion on the vehicle operation has very important significance and practical value. In this paper, investigate the braking process of the vehicle under different influencing factors are prefabricated using rolling contact fatigue tests. Through various analysis methods, the formation mechanism of abrasions and the influence of different abrasions on wheel operation were studied. The result shows that the abrasion area will form a severe plastic deformation layer and a Martensite white layer mainly caused by thermal influence. Running a wheel with abrasion will cause greater wear, and it will have a serious impact on the life of the wheel, and the surface of the scratch area after rolling has different surface damage morphology.

KEYWORDS: wheel abrasion; wheel material; white layer; rolling contact fatigue; temperature

INTRODUCTION

Recently, the development of high-speed rail will pay more attention to technological innovation and technological progress, and use innovation to promote the construction and development of high-speed rail networks [1-8]. The railway transportation has many advantages such as large volume, fast speed, high efficiency, low cost, and stability. The wheel/rail problem has always been one of the critical issues restricting the development of high-speed train technology. Among them, the wheel/rail contact fatigue problem is a very complicated and interdisciplinary scientific problem, which includes tribology, materials science, and heat transfer. The abrasion problem is a frequent and very serious wheel/rail damage problem in a wheel/rail system [9].

Many researchers have also observed a large number of white layers on the contact surfaces of the rails and wheels. The concept of "white layer" was first discovered and proposed by Stead on wire ropes in 1912, and it is generally easy to appear on the surface of bearing balls, brake discs and gun barrels. The formation of these white layers It appears when there are frictional conditions between the interfaces, and this type of white layer is also reduced to the tribological white layer [10]. At the same time, the white layer may also appear on the surface of the non-friction interface. For example, the laser-enhanced workpiece surface is extremely prone to appear on the surface of the workpiece [11]. Also, it is easy to observe the white layer on the cutting surface when cutting the sample using EDM Existence. It is precisely because the white layer frequently appears in the engineering site and laboratory conditions, so there are a lot of researches on the white layer. However, the research on the white layer is still controversial and many problems that require further study [12], this article mainly Some research is done on the white layer appearing in the wheel-rail test. This is due to the high contact stress and certain frictional conditions between the wheel and rail contact interfaces. At the same time, since the material of wheel rails is mainly pearlite steel. These common factors are the reasons why a white layer is easily formed between the wheel-rail contact interface. Many studies have also shown that in the actual wheel-rail system, the rails are more likely to have a white layer, which is also related to the characteristics of long-term service of the rails. Also, this white layer happens especially in the curved section and the corrugated rails, the appearance of the white layer of rails [13]. The appearance frequency of the wheel white layer is relatively less than the previous study. The wheel white layer is generally related to the occurrence of abrasions on the tread. A large number of abrasion tests can observe the appearance of a white layer in the abrasion area [14].

There are still many problems to be solved in various subjects such as science and dynamics.

In this paper, we mainly focus on analysing the white layer appearing at the wheel abrasions. The analyses of the test results of the control test group, including analysis and summary of the amount of wear, surface hardness before and after the test, and surface morphology. The effect of the presence or absence of abrasion on the running of the wheels was compared and analysed through the test results. At the same time, a white layer was found on the surface of the scratched area of the sample, and the white layer was further analyzed. The nano-hardness measurement and XRD analysis were used to determine the structure and formation mechanism of the white layer. Finally, the formation and evolution of the abrasion were analysed through online observation, and a diagram of the formation and evolution mechanism of the abrasion was drawn according to the evolution process to explain the process and cause of the abrasion of the wheel.

BACKGROUND

The wheel/rail abrasion

Generally, a wheel/rail abrasion is classified into a wheel abrasion and a rail abrasion. This article focuses on wheel abrasion, so only wheel abrasion is introduced. As shown in Figure 1, wheel abrasion often occurs on the rolling surface of the wheel; that is, the wheel tread, which is also commonly referred to as wheel tread abrasion. Many works of literature call it wheel flat scars based on their special shape [15-17].

Figure 1. Wheel tread abrasion [8]

Causes of Wheel Scratches

Although wheel abrasions are more common, the reasons for their formation are various. From the field reasons, they can be roughly summarized into the following categories [18,19]:

(1) The cause of the vehicle itself
(2) Reasons for the operation of the on-site personnel
(3) Operating environment reasons
(4) Reasons for running the route

The main reasons are the formation of wheel abrasions, and the mechanical reasons for the formation of abrasions can be summarized as follows: When the wheel is braking, the braking force exceeds the adhesion between the wheels and the rails, which causes the wheel to be locked in place. Dragging on the rail caused macro sliding between the wheel-rail contact interface. Due to the very large contact stress between the wheel-rail contact interface and the large sliding friction coefficient, a strong mechanical force and generated the interface a large amount of frictional heat removes the material at the contact surface of the wheel under the common action of the two, thereby forming an oval scratch spot. In severe cases, the material will also undergo phase transformation and generate severe thermal cracks. From many literature statistics, it can be analyzed that in the winter and autumn when the track is covered with fallen leaves and water, the brake is prone to abrasion during the running of the locomotive [20], which is due to the temperature and humidity caused by the season and the environment. The change will cause the adhesion coefficient of the wheel and rail to decrease, which will cause the wheel to lock and slip during the braking process, resulting in abrasion. It can be seen that the

abrasion is closely related to the adhesion coefficient between the wheel and rail interface and the braking force.

MATERIAL AND METHODS

In order to study the formation of wheel tread abrasion under different braking parameters and its effect on wheel operation, a series of simulation experiments are designed to explore its laws. The simulation test is mainly carried out on a wheel-rail simulation test machine, using real wheel-rail materials and scale-down samples to try to simulate the actual on-site contact conditions.

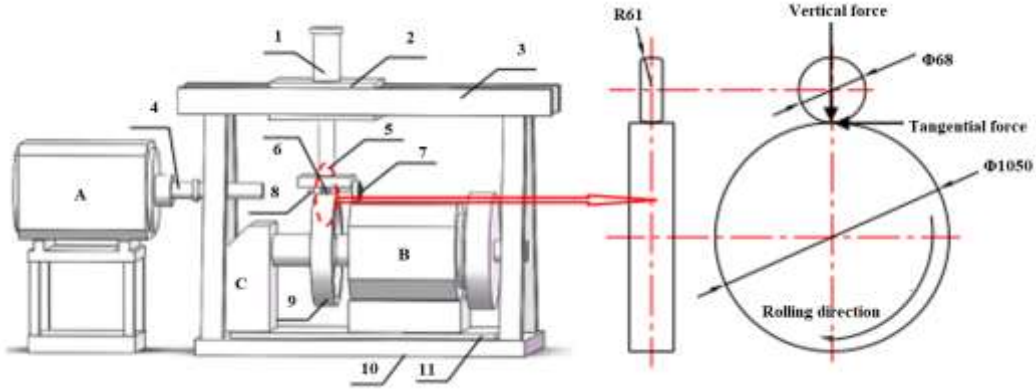

1. Vertical loading hydraulic cylinder; 2. Loading platform; 3. Main body frame; 4. Shaft; 5. Mandrel and yoke; 6. Simulation wheel sample; 7. Magnetic powder brake; 8. Simulation wheel axle; 9. Simulated large wheel; 10. Abutment; 11. Slewing platform; A, B. DC motor; C. Gear box.

Figure 2. Wheel and rail simulation testing machine main structure and sample contact diagram

Test device

The wheel-rail simulation test machine is a large-scale wheel-rail simulation test machine. The test machine is mainly composed of test machine host, hydraulic control system, electronic control system, data acquisition and processing microcomputer system, and simulation of large wheel dressing tools System composition. The main machine of the test machine is mainly composed of abutment, slewing platform, main body frame, loading system, wheel and rail simulation system, drive motor system and gear box, etc. [21]. The schematic diagram of the main structure's contact with the sample of the wheel and rail simulation part is shown in Figure 2. The wheel braking and thermal fatigue test [22]. It also has good results repeatability and reliability.

Selection of test materials

In order to test the accuracy and rigor of the simulation, all the sample materials selected in this test were taken from the wheels on the real site. At the same time, in order to explore the anti-scratch ability of different wheel materials and the anti-fatigue and wear performance of running after abrasion, three different wheel materials were selected for comparison tests. As carbon content is one of the most important factors affecting the performance of steel, three wheel materials with different carbon contents, D2, CL60 and CL70, were selected for comparison. Among them, D2 wheel material was used as the main material in this experiment. And CL70 wheel materials are only used for comparative studies. The rail material used as the control is the simulated large wheel of the wheel-rail simulation test machine. The outer material of the large wheel is made of real steel material and cannot be changed, which also ensures the consistency of the test conditions. All appealing test materials can be found in the table below (Table 1).

Table 1. Chemical composition of wheel and rail samples used in the test (wt.%)

Sample	C	Mn	Si	S	P
D2	≤0.56	≤0.80	≤0.40	≤0.015	≤0.020
CL60	0.57~0.65	≤0.80	≤0.40	≤0.010	≤0.020
CL70	0.67~0.77	0.60~0.90	0.15~1.00	0.005~0.04	≤0.030

Rail	0.62~0.77	1.40	0.15~0.37	≤0.033	≤0.02

The test parameters of this group are shown in Table 2. The three wheel samples were treated differently. Sample F1 was not subjected to the braking test, and only the subsequent fatigue wear test was used as a reference. No damage caused by abrasion defects; samples F2 and F3 both undergo braking tests with the same parameters. The difference is that sample F2 only performs a braking test to analyze the effects of braking abrasion on wheel samples damage; while sample F3 was subjected to subsequent rolling contact wear and fatigue tests after abrasion with the same parameters, the impact of the abrasion formed by this parameter on the wheel operation was analyzed.

Table 2. Control parameters of the control group

Sample No	Wheel to brake	Braking speed (km/h)	Braking time (s)	Wheel to run
F1	×	—	—	√
F2	√	120	10	×
F3	√	120	10	√

Test procedure

The test process is roughly divided into two parts (except for the control group sample F1, which only performs the fatigue wear test, and sample F2, which only performs the brake abrasion test). The first part is the brake abrasion test. This part is mainly for prefabrication. Analysis of the impact of different test parameters on wheel abrasion; the second part is the rolling contact wear and fatigue test, which is mainly to study the running of the wheel with the abrasion defect formed after the wheel has formed abrasion after braking The effects of wheel fatigue life and wheel wear.

The main steps of the first part of the brake abrasion test are as follows:

(1) Install the prepared wheel sample on the wheel-rail simulation test machine according to the test requirements. After the installation is completed, the wheel sample and the simulated large wheel are washed again with alcohol to remove the pollutants during the installation process and ensure the simulation. Cleaning of wheel and rail contact surfaces;
(2) Start the large wheel motor of the testing machine, then load the vertical load to 120kg, and gradually adjust the speed of the large wheel to 100rpm. All the samples are run in under this parameter for 5min to ensure the stability of the system and contact interface;
(3) After the brake test is completed, the wheel sample is subjected to the fatigue wear test with abrasion defects. After adjusting the vertical load and the wheel speed according to the target value, adjust the current of the magnetic powder brake controller to 10%. The rotation of the sample provides a certain braking torque to simulate the friction existing in the field;
(4) The subsequent rolling contact wear and fatigue test of the sample requires the wheel sample to be stopped for observation after every 20,000 cycles. The wheel sample is also observed and recorded with a portable microscope without disassembly, so that the friction can be compared. Change pattern of injured specimen surface during wheel running;
(5) The wheel sample is stopped after 100,000 cycles to save the test data. The wheel sample is removed and the surface is recorded with a portable microscope. Then, the sample is washed and weighed to obtain the wheel wear amount of the test. After the completion, the sample is placed in a sample bag and sealed, stored dry to prevent oxidation, and used for subsequent sampling and analysis.

After the test is completed, the abrasion area of the wheel sample is sampled and analyzed. The sampling method is shown in Figure 3. Use a marker pen to mark (the cutting area of the abrasion area 2mm, cutting depth 5mm), use a wire cutter to cut and remove the area, cut the sample block along the center line, and then analyze the removed sample as follows:

(1) Put the sample in an ultrasonic cleaner for cleaning, and then dry it with a hair dryer. Use an optical microscope (OLYMPUS BX60M) and a scanning electron microscope (JSM-7001F) to observe and analyze the surface morphology of the sample, and use XRD analysis of some samples;
(2) After the above analysis is completed, the sample is inlaid with resin, the section of the sample is ground and polished, and the crack and damage of the sample section are observed and recorded with an optical

microscope, and then the section is subjected to a 5% nitric acid alcohol solution. Carry out corrosion treatment, observe and record the microstructure, plastic deformation and section damage of the section with an optical microscope and a scanning electron microscope;

(3) Finally, the surface hardness and section hardness of the abraded area were measured with a Vickers hardness tester. Some samples were measured for nanohardness on the section with a nanohardness tester (Agilent G200), and the laws were analyzed.

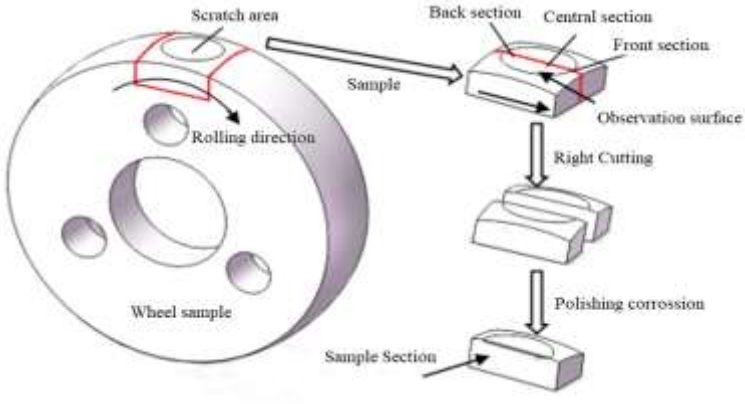

Figure 3. Sampling diagram of the scratched area of the wheel sample

RESULT AND DISCUSSION

Wear and surface damage characteristics

Figure 4 shows the wear of each wheel specimen after the control group test. It can be seen from the figure that from sample F1 to F3, the amount of wear increases sequentially, and the increase is larger. Careful analysis of the amount of wear of each sample can be found: Wheel sample F1 did not undergo any special treatment in the test, only the conventional rolling contact wear and fatigue test was performed, and its wear was extremely small after 100000 cycles of rolling (0.099g); while the sample F2 was only subjected to abrasion treatment, and subsequent rolling contact wear and fatigue tests were not performed, the wear amount was 0.363g. By comparing the amount of wear of samples F1 and F2, it can be found that the amount of wear of sample F2 is more than 3.6 times that of sample F1, which indicates that the amount of wear caused by surface abrasion of the wheel sample is much larger than that caused by normal operation of the wheel The amount of wear caused is that when the wheel is abraded due to braking, a large abrasion area is formed on the sample surface. The abrasion process is a rapid and violent material removal process, so the volume of material removed by it is much larger than the normal running wear of the wheel, which causes the wear of sample F2 to be much larger than that of F1. Analysis of the wear amount of wheel sample F3 shows that the wear amount of 0.716g is greater than the wear amount of sample F2 of 0.363g. This is because sample F3 was subjected to subsequent rolling contact wear and friction after pre-scratching with the same parameters as F2. In the fatigue test, the running of the sample caused the wear of the sample, so the wear of sample F3 is greater than that of F2. Further analysis of the wear amount of the three samples can be found: The wear amount of the sample F1 (only fatigue wear test) and F2 (only abrasion test) are superimposed, that is, 0.099g + 0.363g = 0.462g, The sum of the abrasion amount is less than the abrasion amount of sample F3 by 0.716g (about 1.5 times the sum of the former two), and from the test parameters, it is known that the sample F3 is scratched with the same parameters as F2. F1 parameters are consistent with rolling contact wear and fatigue tests. This result shows that the running of the specimen after abrasion also has a great effect on its wear. The running of the wheel after abrasion will aggravate its running wear. This is because the original outer geometry of the sample was changed after the wheel was abraded, and a flat scar was formed at the position of the abrasion area. When the wheel abrasion area passed the rail, a certain impact was formed here. The extent to which the wheel wears. Finally, from the analysis of the sample wear in the figure, it can be known that the abrasion itself will increase the wheel wear, and at the same time, the running wear of the wheel will increase after the abrasion, resulting in a large increase in the wear.

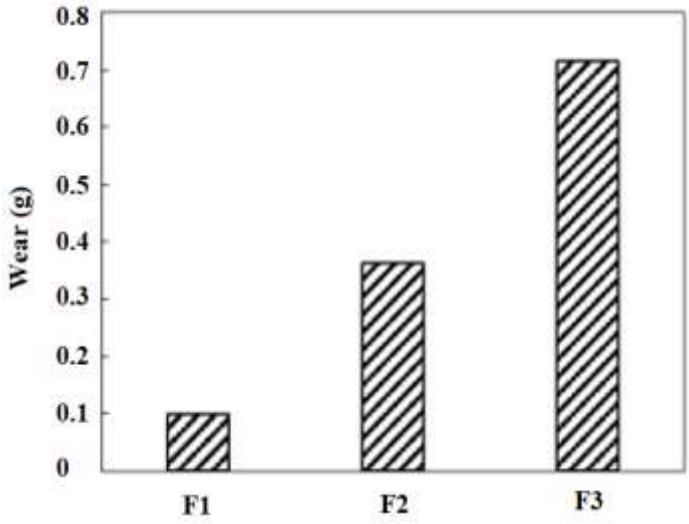

Figure 4. Abrasion of wheel samples in the control group

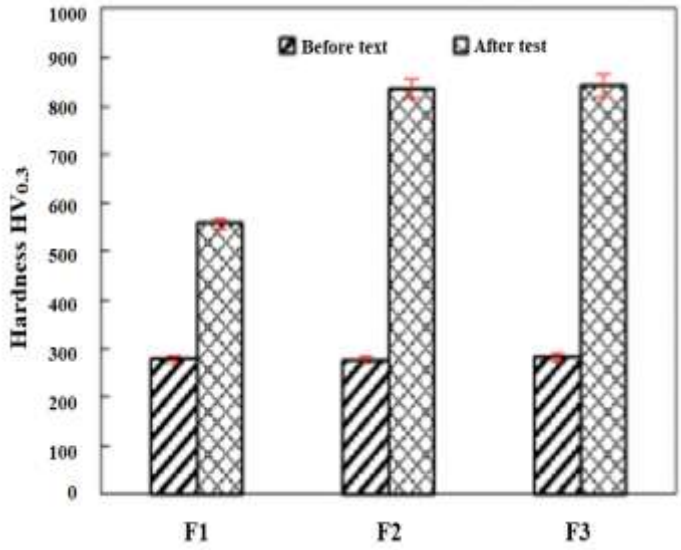

Figure 5. Surface hardness before and after the test

Figure 5 shows the comparison of the surface hardness before and after the test in the abrasion zone of the wheel sample of the control group (except for sample F1). The pre-test hardness of each sample uses the average value of the surface hardness measured during the test before the test, which can be seen: the surface hardness of all wheel specimens was basically the same before the test, and the Vickers hardness values were maintained at about 280$HV_{0.3}$. The red marks in the figure are the error bands. The error is small because the surface of the wheel specimens was processed uniformly and smooth before the test. The comparison shows that the surface hardness values of the scratched areas of samples F2 and F3 are relatively close to 836$HV_{0.3}$ and 842$HV_{0.3}$, respectively, but the values are much higher than the surface hardness of sample F1. This hardness value can indicate: The microstructure evolved and the hardness reached the hardness of the white martensite layer. This is because when the wheel is locked during braking, the wheel slides on the surface of the rail and it is very easy to generate high temperature, so that a white layer is formed in the area of surface abrasion. It is easy to form a white layer on the abrasion of the wheel tread, and its surface hardness will generally exceed 800 $HV_{0.3}$, and the surface hardness value of general wheel rail materials after plastic deformation cannot reach this hardness range. The surface material structure has undergone plastic deformation, which is commonly referred to as work hardening [23], so its surface hardness increases. This value is also the hardness value of a typical wheel surface after plastic deformation.

Figures 6, 7, and 8 are the surface damage maps of the three samples of the control group. In order to facilitate

the observation and comparison of the test rules, except for sample F1, which has no abrasion zone, the other specimens with abrasion zone will define the abrasion zone as the rear, middle and Front (the direction of the arrow shown in the figure is the front of the abrasion area).

Figure 6 is the surface damage map of sample F1. From Figure 6 (a), it can be seen that because sample F1 has only been subjected to the conventional rolling contact fatigue test, no other special treatment has been performed, and its surface has not appeared. Abnormal damage after zooming in on a part of it (Figure 6 (b)), it can be seen that the surface of sample F1 is mostly small peeling pits and some peeling and peeling, which are all minor damage caused by typical wheel fatigue tests. Damage does not have an abnormal effect on the life of the wheel and belongs to the normal range of fatigue damage.

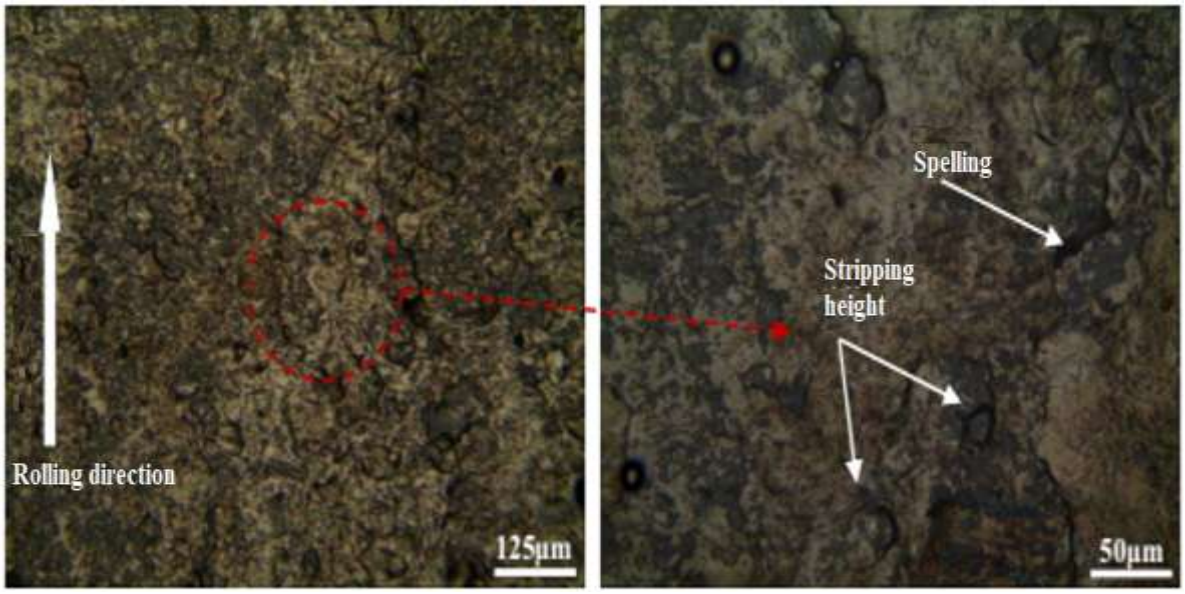

(a) Surface wear scars (b) Local enlargement

Figure 6. Surface morphology of specimen F1

Sample F2 was subjected to abrasion test, so the abrasion area was selected for observation. Figures 7 (a) and (b) show the front surface morphology of the abraded area of sample F2. It can be seen that: the middle blue dotted line shows the boundary of the abrasion area. This is due to the sliding between the wheel sample and the rail sample during the abrasion process. Under severe mechanical and thermal effects, the material on the contact surface of the wheel sample was removed. A flat scar was formed, so a clear boundary line appeared between it and the surrounding surface, and some furrows and flaking occurred due to the sliding between the interfaces.

Figure 7 (c) and (d) are the topography of the middle surface of the abrasion zone of the sample F2. It can be seen that the middle surface damage of the abrasion zone is mainly manifested by a large number of furrows parallel to the rolling direction, mainly due to When the rail sample brakes, the sliding occurs at the contact interface of the wheel abrasion area to form a very strong mechanical effect. The tiny bumps between the contact interface cause the wheel material to scratch, thereby forming a lot of furrow damage.

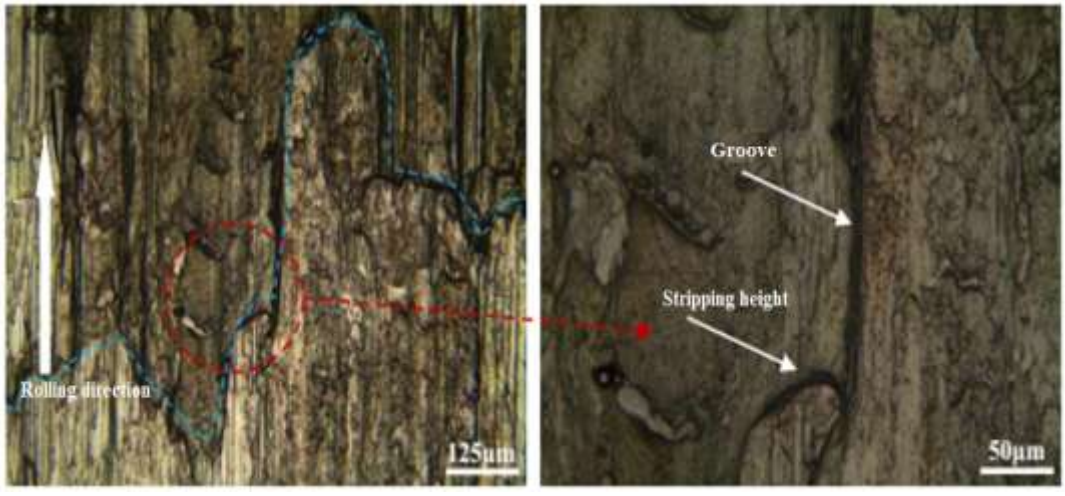

(a) Topography of the abrasion area (b) Topography of the abrasion area

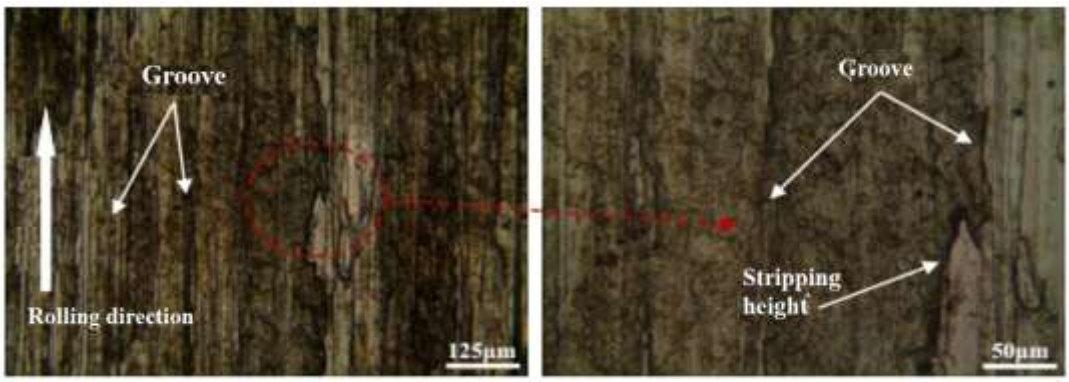

(c) Surface morphology in the middle of the abrasion area

(d) Surface morphology in the middle of the abrasion area

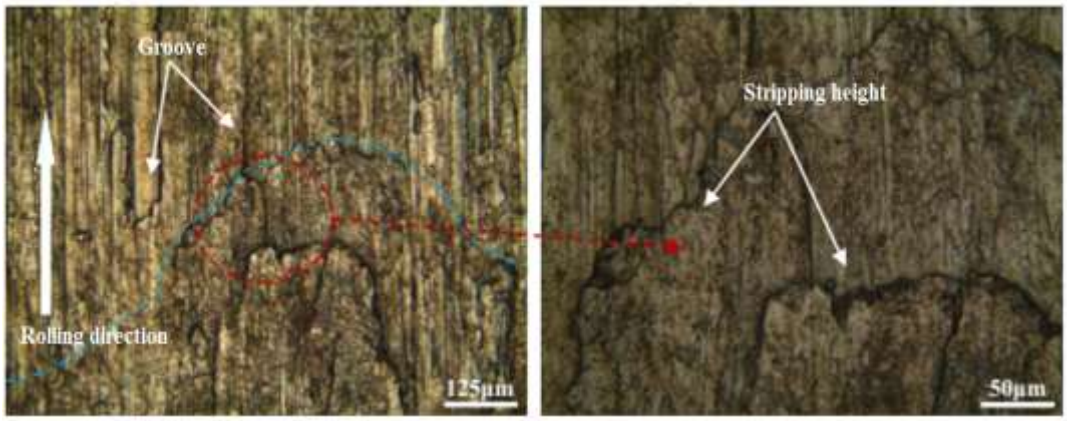

(e) Topography of the abrasion area (f) Topography of the abrasion area

Figure 7. Surface damage morphology of the abrasion zone of specimen F2

Figures 7 (e) and (f) show the top surface morphology of the abrasion zone of sample F2. The blue dotted line in Figure 7 (e) is the rear boundary of the abrasion zone. The reason for formation is the same as the formation of the front boundary of the abrasion zone, but it is also formed in the rear due to the effect of strong mechanical action during sliding. Some furrows and material were stripped. Because the same sample F3 also

forms a brake sample with the same parameters as F2, their morphology of the abrasion area has certain similarities.

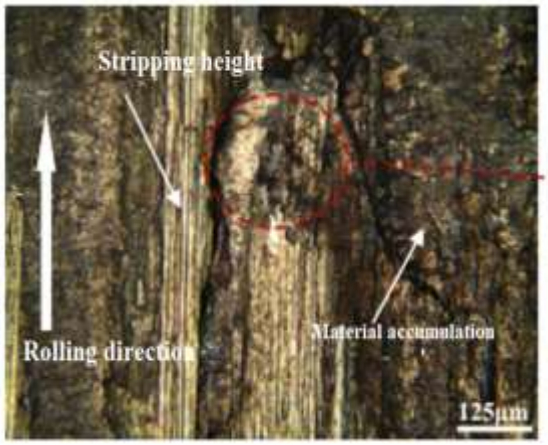

(a) Topography of the abrasion area

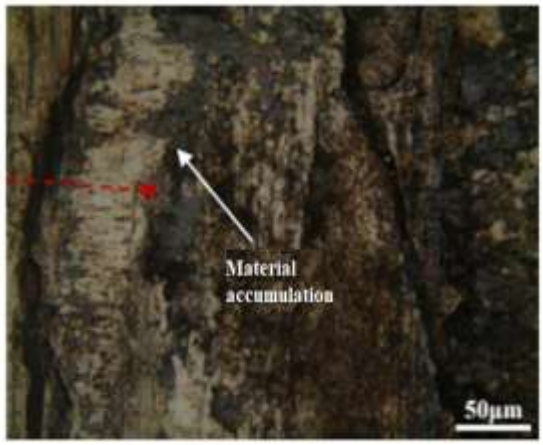

(b) Topography of the abrasion area

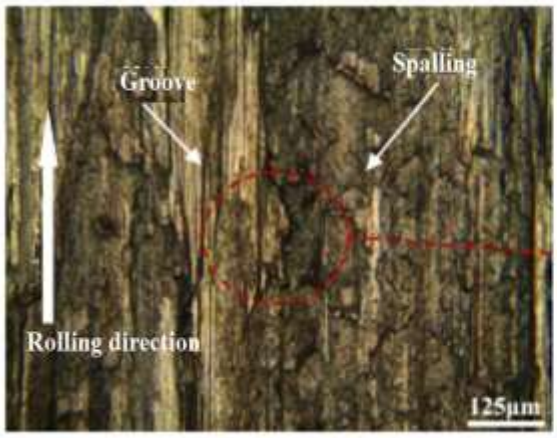

(c) Surface morphology in the middle of the abrasion area

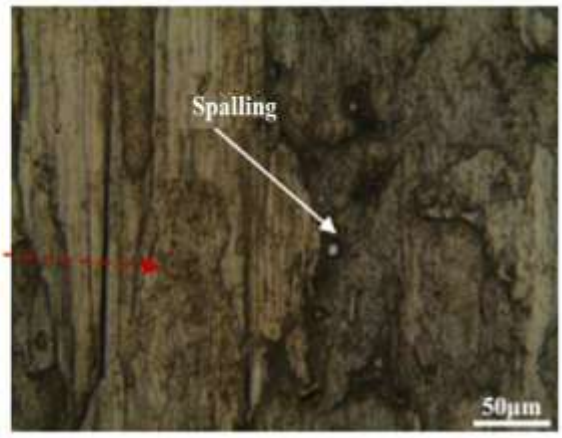

(d) Surface morphology in the middle of the abrasion area

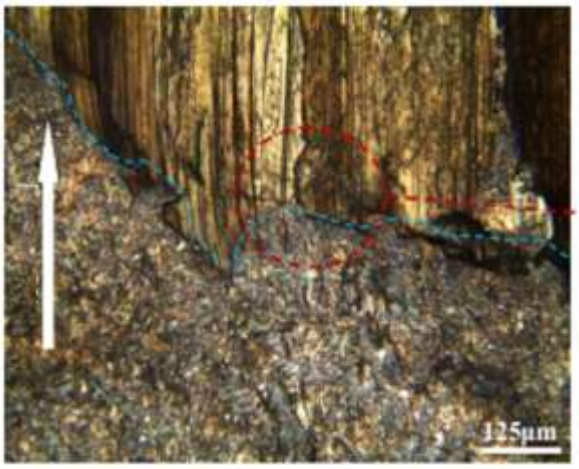

(e) Topography of the abrasion area

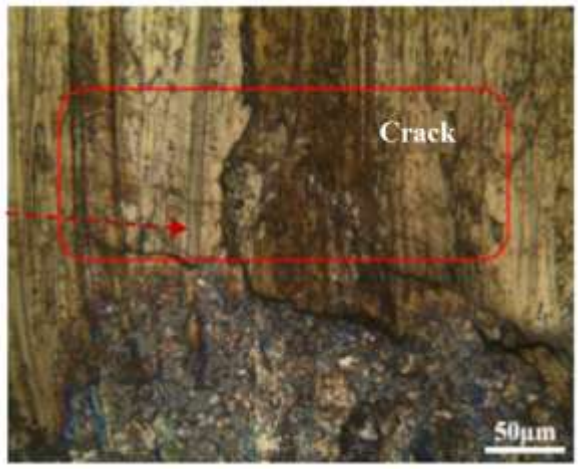

(f) Topography of the abrasion area

Figure 8. Surface damage of the scratched area of specimen F3

As shown in Figure 8, the front of the abrasion area of sample F3 is the same. A clear boundary line (shown by the blue dashed line in the figure) is also formed at the rear and the rear. The reason for formation is the same as that of sample F2, and the damage in the middle of the abrasion area is also the same as that of sample F2. The damage was mainly accompanied by a small amount of peeling damage. The difference between sample F3 and sample F2 in the abrasion area is that sample F3 has a large amount of material accumulation in the front of the abrasion area. This is because sample F3 was subjected to a rolling contact fatigue test after the abrasion test. In the subsequent rolling process, the outer shape of the wheel lost part of the material after abrasion, which caused the wheel to be out of shape. During the rolling process, the front part of the abrasion area was in contact with the rails. Certain material builds up. Sample F3 showed a lot of surface cracks and severe peeling at the rear of the abrasion area, which was caused by a large impact when the wheel contacted the rail sample after the abrasion area was not round. By comparing the surface damage of the samples F1 and F2, it can be seen that the damage of the abrasion to the wheel is far greater than that of normal rolling operation. The abrasion can cause serious defects on the surface of the wheel in a short time, forming a more serious Destructive form. By comparing the surface damage of the samples F2 and F3, it can be seen that the running of the wheel after the formation of abrasion will aggravate the surface damage of the wheel, the more serious damage such as material accumulation and surface cracks forming the abrasion area, so the wheel is abraded will seriously affect the running of the wheels.

White layer analysis of abrasions

In order to more accurately determine the hardness gradient in the white layer profile area, the nanohardness of the white layer, the transition layer, and the plastic deformation layer of the sample was then measured using a nanohardness meter. Figure 9 shows the measured nanohardness of the three layers of the white layer, transition layer, and plastic deformation layer are 12.6GPa, 7.3GPa, and 5.9GPa, respectively. The hardness of the white layer is also the same as that of previous scholars. The measured hardness of the white layer [24]. Because the transition layer is a mixed layer of white layer structure and ferrite, its hardness value is also higher than that of the plastic deformation layer. The hardness value from the section also shows that the white layer formed in the test should be a white layer.

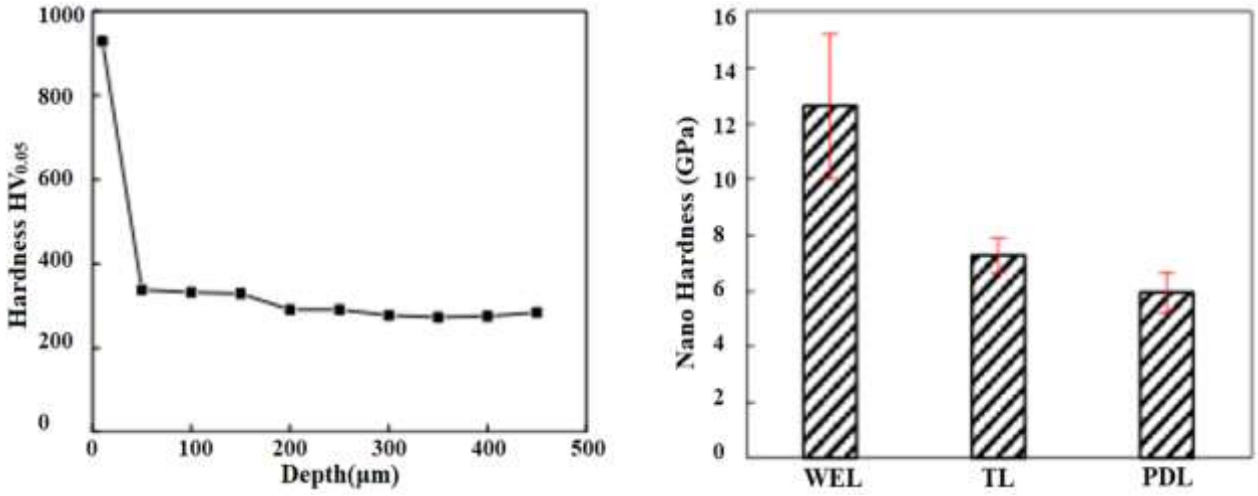

(a) Dimensional hardness of the scratched area (b) Nano hardness of the scratched area

Figure 9. Cross-section hardness of the scratched area of the wheel specimen

XRD composition

In order to further prove that the white layer formed in the abraded area in the test is a white layer, an X-ray diffraction analysis (XRD) was performed on the abraded area of the sample to determine the composition of the abraded area structure. The XRD analysis results of the injury area are used for comparison. Figure 10 is the XRD result map, where black represents the scan result of the abraded area, and red represents the result of the abraded area. Enlarging the area of 40°~50° shows that martensite and austenite exist in the tissue of the

abraded area. And no abrasions in these areas. Combined with the surface and section hardness values of the abraded area in the previous section, it can be determined that the white layer that appears in the sample is the white layer. And because the existence of residual austenite was found in the XRD analysis, this can prove that the formation mechanism of the white layer formed in this test is formed by the influence of heat, not by the plastic mechanism, only under the influence of heat martensite formed under the mechanism will have residual austenite [25-27].

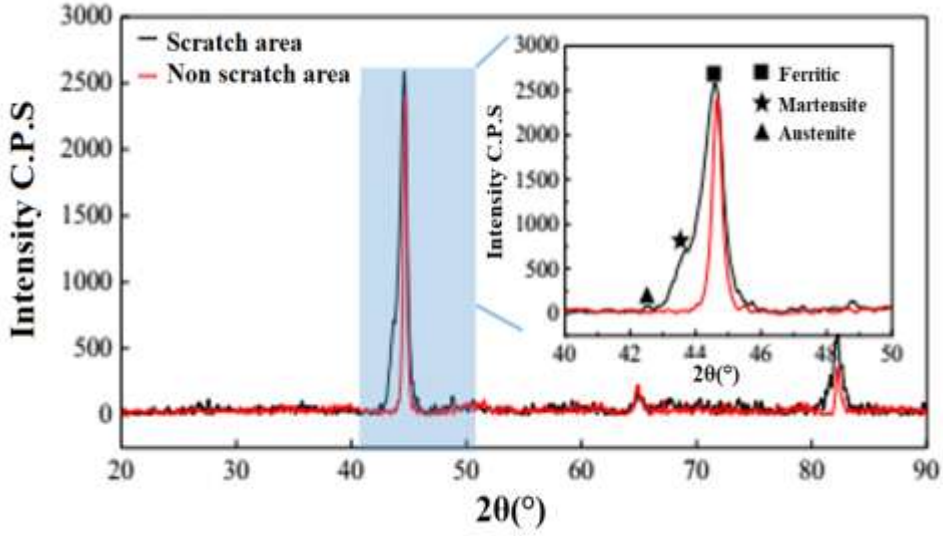

Figure 10. XRD comparison chart of the scratched and unscratched areas of the wheel sample

Diagram of abrasion evolution mechanism

According to the test results and analysis of the appeal, in order to more intuitively show the formation process of the wheel abrasion and the influence rule of the abrasion on the wheel operation, the abrasion effect mechanism diagram of Figure 11 was drawn. Figure 11 (a) shows the process of abrasion formation. Wheels are locked during emergency braking, which causes sliding between the wheel-rail interface. Under strong mechanical action, the surface tissue of the abrasion area undergoes severe plastic deformation. At the same time, the heat generated by the friction caused the temperature of the abrasion zone to rise sharply, causing the surface structure to undergo a phase change, forming a white layer [28]. Wheel abrasion damages the wheel's geometry and forms a flat surface. As shown in Figure 11 (b), when the wheel continues to roll again, the front of the abrasion area is in contact with the rails. Because the edge of the abrasion area forms a sharp corner, stress occurs at the sharp corner, which makes the rubbing. The material at the front of the scratch area is squeezed to both sides, and continuous rolling and squeezing causes the material to accumulate there [29]. This phenomenon can also be observed in the above test results. As shown in Figure 11 (c), after the wheel comes into contact with the front of the abrasion, the wheel takes off due to the rotating inertia. The middle of the abrasion area and the contact surface of the rail briefly separate, and then the wheel continues to rotate and falls, forming a large impact on the back of the abrasion zone [30] (Fig. 11 (d)), this impact causes the original small thermal cracks to expand, and due to the brittleness of the white layer Under the influence of external force, the white layer at the back of the abrasion area is easily broken to form cracks. These cracks further expand to the substrate under this continuous impact, and finally form more severe long cracks, which seriously affects the service life of the wheel and even affects Driving safety, this is also the reason why larger angle cracks can be observed at the rear of the abrasion area after the test.

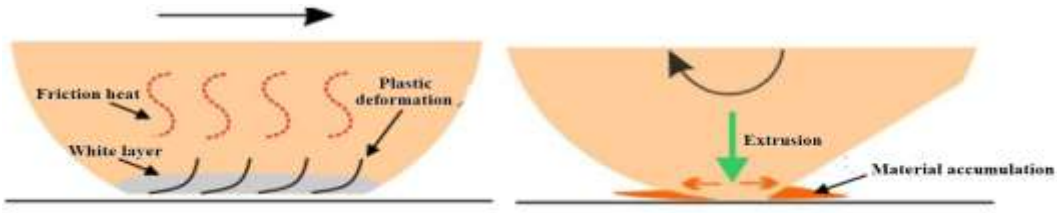

(a) Scratch formation (b) Front squeezing

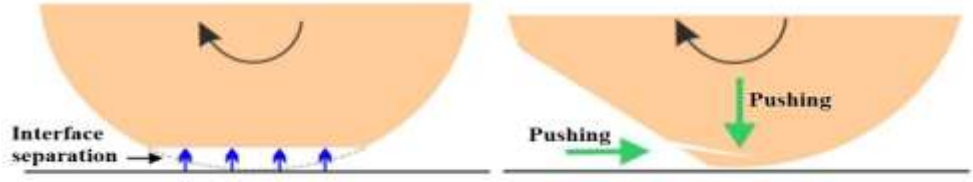

(c) Central separation (d) Rear impact

Figure 11. Mechanism of scratch formation and operation process

CONCLUSION

Through the control group test in this chapter, the influence of the tread abrasion itself on the running of the wheel is analyzed. At the same time, the detailed analysis of the white layer formed on the surface layer of the abrasion area and the analysis of the formation and evolution of the abrasion through online observation, the following main conclusions were reached:

(1) The abrasion itself will increase the amount of wheel wear. At the same time, running after abrasion will increase the wear of the wheel, causing a large increase in the amount of wear. At the same time, the wheel abrasion will also cause severe plastic deformation in the abrasion area, and Severe hardening of the surface of the abrasion area;
(2) After the wheel is abraded, a white layer structure will be formed in the abrasion area, and the white layer structure is mainly martensite. It is known that the white layer in the abrasion area is mainly caused by thermal influence of residual austenite in its composition.
(3) Running after abraded wheels will severely affect the life of the wheels, and different surface damage morphologies are formed in the front, middle, and rear parts of the abraded area after rolling. The front part of the abraded area is mainly material accumulation, and the middle part is mainly for furrows and spalling, the rear part is mainly a surface crack, and a severe crack with a large angle and spreading to the substrate will appear at the rear part of the abrasion area.

ACKNOWLEDGMENTS

The authors would like to thank Tikrit University and Universiti Malaysia Pahang for providing laboratory facilities and financial support.

REFERENCES

[1] T.K. Ibrahim, M.K. Mohammed, O.I. Awad, A.N. Abdalla, F. Basrawi, M.N. Mohammed, G. Najafi, and R. Mamat, "A comprehensive review on the exergy analysis of combined cycle power plants", *Renewable and Sustainable Energy Reviews*, vol. 90, pp. 835-850, 2018.

[2] T.K. Ibrahim, M. Marwah Noori, and I. Hassan, "Effect of perforation area on temperature distribution of the rectangular fins under natural convection", *ARPN Journal of Engineering and Applied Sciences*, vol. 11, pp. 6371-6375, 2016.

[3] T.K. Ibrahim, M.N. Mohammed, M. Kamil Mohammed, G. Najafi, N. Azwadi Che Sidik, F. Basrawi, A.N. Abdalla, and S.S. Hoseini, "Experimental study on the effect of perforations shapes on vertical heated fins performance under forced convection heat transfer", *International Journal of Heat and Mass Transfer*, vol. 118, pp. 832-846, 2018. Doi: https://doi.org/10.1016/j.ijheatmasstransfer.2017.11.047.

[4] M.N. Mohammed, K.B. Yusoh, and J.H.B.H. Shariffuddin, "Methodized depiction of design of experiment for parameters optimization in synthesis of poly (Nvinylcaprolactam) thermoresponsive polymers. *Materials Research Express*, vol. 3, pp. 125302, 2016.

[5] M.N. Mohammed, K.B. Yusoh, and J.H.B.H. Shariffuddin, "Parametric Optimization of the Poly (Nvinylcaprolactam)(PNVCL) Thermoresponsive Polymers Synthesis by the Response Surface Methodology and Radial Basis Function neural network", In Proceedings of MATEC Web of

Conferences, pp. 02023.

[6] M.N. Mohammed, K.B. Yusoh, and J.H.B.H. Shariffuddin, "Poly (N-vinyl caprolactam) thermoresponsive polymer in novel drug delivery systems: A review", *Materials Express*, vol. 8, pp. 21-34, 2018.

[7] M.N. Mohammed, K.B. Yusoh, M.N. Ismael, and J.H.B.H. Shariffuddin, "Synthesis of thermo-responsive poly (N-vinylcaprolactam): RSM-based parameters optimization", *Multiscale and Multidisciplinary Modeling, Experiments and Design*, pp. 1-9, 2019.

[8] T.K. Ibrahim, and M.N. Mohammed, "Thermodynamic evaluation of the performance of a combined cycle power plant", *International Journal of Energy Science and Engineering*, vol. 1, pp. 11, 2015.

[9] C.P. Liu, P.T. Liu, J.Z. Pan, C.H. Chen, and R.M. Ren, "Effect of pre-wear on the rolling contact fatigue property of D2 wheel steel", *Wear*, pp. 442-443, 203154, 2020. Doi: https://doi.org/10.1016/j.wear.2019.203154.

[10] Y. Hu, L. Zhou, H.H. Ding, G.X. Tan, R. Lewis, Q.Y. Liu, J. Guo, and W.J. Wang, "Investigation on wear and rolling contact fatigue of wheel-rail materials under various wheel/rail hardness ratio and creepage conditions", *Tribology International*, vol. 143, pp. 106091, 2020. Doi: https://doi.org/10.1016/j.triboint.2019.106091.

[11] T.X. Wu, and D.J. Thompson, "A Hybrid Model for The Noise Generation Due to Railway Wheel Flats", Journal of Sound and Vibration, vol. 251, pp. 115-139, 2002. Doi: https://doi.org/10.1006/jsvi.2001.3980.

[12] J. Seo, S. Kwon, H. Jun, and D. Lee, "Numerical stress analysis and rolling contact fatigue of White Etching Layer on rail steel", *International Journal of Fatigue*, vol. 33, pp. 203-211, 2011.

[13] S. Grassie, "Rail corrugation: characteristics, causes, and treatments. Proceedings of the Institution of Mechanical Engineers", Part F: *Journal of Rail and Rapid Transit*, vol. 223, pp. 581-596, 2009.

[14] R. Belli, C. Rahiotis, E.W. Schubert, L.N. Baratieri, A. Petschelt, and U. Lohbauer, "Wear and morphology of infiltrated white spot lesions", *Journal of Dentistry*, vol. 39, pp. 376-385, 2011.

[15] A. Zagame, "Flexible adhesive element for external medical use in the treatment of hypertrophic or cheloid scars following breast surgery", *Google Patents*, 1999.

[16] T.S. Alster, and T.B. West, "Treatment of scars: a review. *Annals of Plastic Surgery*, vol. 39, pp. 418-432, 1997.

[17] D. Fu, W. Wang, and L. Dong, "Analysis on the fatigue cracks in the bogie frame", *Engineering Failure Analysis*, vol. 58, pp. 307-319, 2015.

[18] C.G. He, Y.Z. Chen, Y.B. Huang, Q.Y. Liu, M.H. Zhu, and W.J. Wang, "On the surface scratch and thermal fatigue damage of wheel material under different braking speed conditions", *Engineering Failure Analysis*, vol. 79, pp. 889-901, 2017. Doi: https://doi.org/10.1016/j.engfailanal.2017.06.017.

[19] X. Yang, Z. Qiu, and X. Li, "Investigation of scratching sequence influence on material removal mechanism of glass-ceramics by the multiple scratch tests", *Ceramics International*, vol. 45, pp. 861-873, 2019. Doi: https://doi.org/10.1016/j.ceramint.2018.09.256.

[20] B. Li, "Three-Dimensional Stress Field Analysis of Brake Shoe for Locomotives during Braking Process", *Recent Patents on Mechanical Engineering*, vol. 9, pp. 48-56, 2016.

[21] H.W. He, F.C. Sun, and J. Xing, "Dynamic simulation and experiment of electric drive system on test bench", In Proceedings of 2007 IEEE International Conference on Vehicular Electronics and Safety, pp. 1-4.

[22] A. Mazzù, L. Provezza, N. Zani, C. Petrogalli, A. Ghidini, and M. Faccoli, "Effect of shoe braking on wear and fatigue damage of various railway wheel steels for high speed applications", *Wear*, pp. 434-435, 203005, 2019. Doi: https://doi.org/10.1016/j.wear.2019.203005.

[23] A. Torkestani, and M.R. Dashtbayazi, "A new method for severe plastic deformation of the copper sheets", *Materials Science and Engineering: A*, vol. 737, pp. 236-244, 2018. Doi: https://doi.org/10.1016/j.msea.2018.09.054.

[24] Y. Zhou, J.F. Peng, Z.P. Luo, B.B. Cao, X.S. Jin, and M.H. Zhu, "Phase and microstructural evolution in white etching layer of a pearlitic steel during rolling–sliding friction", *Wear*, vol. 362-363, pp. 8-17, 2016. Doi: https://doi.org/10.1016/j.wear.2016.05.007.

[25] A.M. Ravi, A. Navarro-López, J. Sietsma, and M.J. Santofimia, "Influence of martensite/austenite interfaces on bainite formation in low-alloy steels below Ms", *Acta Materialia*, vol. 188, pp. 394-405, 2020. Doi: https://doi.org/10.1016/j.actamat.2020.02.003.

[26] J. Hidalgo, K.O. Findley, and M.J. Santofimia, "Thermal and mechanical stability of retained austenite surrounded by martensite with different degrees of tempering", *Materials Science and Engineering: A*, vol. 690, pp. 337-347, 2017. Doi: https://doi.org/10.1016/j.msea.2017.03.017.

[27] F.R. Kaschel, R.K. Vijayaraghavan, A. Shmeliov, E.K. McCarthy, M. Canavan, P.J. McNally, D.P. Dowling, V. Nicolosi, and M. Celikin, "Mechanism of stress relaxation and phase transformation in additively manufactured Ti-6Al-4V via in situ high temperature XRD and TEM analyses", *Acta Materialia*, vol. 188, pp. 720-732, 2020. Doi: https://doi.org/10.1016/j.actamat.2020.02.056.

[28] R. Pan, R. Ren, C. Chen, and X. Zhao, "The microstructure analysis of white etching layer on treads of rails", *Engineering Failure Analysis*, vol. 82, pp. 39-46, 2017. Doi: https://doi.org/10.1016/j.engfailanal.2017.06.018.

[29] A. Sackfield, D. Dini, and D.A. Hills, "Contact of a rotating wheel with a flat. *International Journal of Solids and Structures*, vol. 44, pp. 3304-3316, 2007. Doi: https://doi.org/10.1016/j.ijsolstr.2006.09.025.

[30] M. Wallentin, H.L. Bjarnehed, and R. Lundén, "Cracks around railway wheel flats exposed to rolling contact loads and residual stresses", *Wear*, 258, 1319-1329, 2005. Doi: https://doi.org/10.1016/j.wear.2004.03.041.